

Evaluation of internal actions in tunnel lining applying genetic algorithms to monitoring data

*Original*

Evaluation of internal actions in tunnel lining applying genetic algorithms to monitoring data / Bertagnoli, G.; Marino, F.. - In: IOP CONFERENCE SERIES: MATERIALS SCIENCE AND ENGINEERING. - ISSN 1757-8981. - ELETTRONICO. - 603:(2019), p. 052043. (Intervento presentato al convegno 4th World Multidisciplinary Civil Engineering-Architecture-Urban Planning Symposium, WMCAUS 2019 tenutosi a Prague nel 17-21 June 2019) [10.1088/1757-899X/603/5/052043].

*Availability:*

This version is available at: 11583/2776915 since: 2020-01-03T14:03:36Z

*Publisher:*

Institute of Physics Publishing

*Published*

DOI:10.1088/1757-899X/603/5/052043

*Terms of use:*

This article is made available under terms and conditions as specified in the corresponding bibliographic description in the repository

*Publisher copyright*

(Article begins on next page)

PAPER • OPEN ACCESS

## Evaluation of internal actions in tunnel lining applying genetic algorithms to monitoring data

To cite this article: Gabriele Bertagnoli and Francesco Marino 2019 *IOP Conf. Ser.: Mater. Sci. Eng.* **603** 052043

View the [article online](#) for updates and enhancements.

# Evaluation of internal actions in tunnel lining applying genetic algorithms to monitoring data

Gabriele Bertagnoli<sup>1</sup>, Francesco Marino<sup>1</sup>

<sup>1</sup>Politecnico di Torino, DISEG, Corso Duca degli Abruzzi, 24, Torino, Italy

[gabriele.bertagnoli@polito.it](mailto:gabriele.bertagnoli@polito.it)

## Abstract.

This article presents an algorithm that can be applied to an innovative diagnostic systems for tunnels based on small and low-cost sensors that can be placed inside the tunnel lining and are able to provide the user with real-time information on the state of health of the structure. The aim of the system is measuring the internal actions (axial force, bending moment and shear) and the ovalization of the lining because of the actions exchanged between the ground and the lining itself. The algorithm presented in this paper aims to calculate the forces acting on tunnel lining starting only from the quantities measured by a set of clinometers and pressure sensors placed inside the casting, without any other knowledge of geotechnical or geological parameters. This method can therefore be applied in parallel with other traditional geotechnical investigation tools such as borehole inclinometers and radar interferometry when unexpected actions as landslides are interesting a tunnel.

## 1. Introduction

The design of modern infrastructures, both for road and railway transport, is today oriented to the realization of underground structures, such as tunnels, more than in the past. The reduction of the cost of tunnel excavation, because of the widespread use of tunnel boring machines (TBM) and ecology issues as the protection of landscape and noise reduction have significantly increased the use of tunnels instead of viaducts or other solutions in modern transportation engineering.

Tunnel excavation is nevertheless a procedure that faces the designer to many unknowns, mainly because of the high variability of geological and geotechnical parameters that may be found during the realization [1-3]. The cost related to the realization of extended investigation campaigns in the design phase typically leads to the assumption of higher risks [4-6] and therefore higher safety coefficients, respect to other civil engineering structures such as buildings or bridges.

Monitoring of tunnels during excavation is today a standard approach, but structural health monitoring of this structures throughout the complete service life is not a widespread technique.

During the last decade, the evolution of low cost sensors derived from TLC industry, the development of high-speed internet communication, the birth of cloud based services and the rise of big data platforms able to apply artificial intelligence techniques, have changed the possible applications of structural monitoring that can now be deployed on large scale to infrastructures as a standard option [7-9].



## 2. State of the art

The loads applied by the ground pressure, and, as a consequence, the internal actions in concrete tunnel lining are most of the times not known with accuracy [10-11]. Linear or nonlinear numerical modelling softwares for advanced geotechnical analysis of soil, rock, groundwater, and ground support like FLAC [12] or RS2 [13] provide good help in the estimation of the state of stress, but their solutions are affected by the uncertainty in the input data, which are most of the time known only with fair approximation.

The thrust acting on the lining may differ significantly from the design hypothesis especially when landslides are present or are generated or re-activated by the excavation of the tunnels. In such cases big damage to the structure may occur [14-15] and expensive traditional monitoring systems are generally used [16].

## 3. Description of the monitoring system

The work described in this paper is based on the installation of an innovative monitoring system inside the tunnel lining. The installation procedure is optimized for prefabricated segmental lining system where it is done in factory during the prefabrication of the segments, but can also be realized during the construction of the concrete lining if traditional excavation is used.

The monitoring system is based on a set of MEMS inclinometers and pressure sensors. Each ring section can be equipped by a high number of sensors (as shown in figure 1) as their cost is much lower than traditional laboratory instruments. The clinometers measure the rotation of the lining due to transverse ovalization, whereas the pressure sensors placed inside concrete can measure both axial force and bending moment as more than two of them are placed within the thickness of the concrete wall.

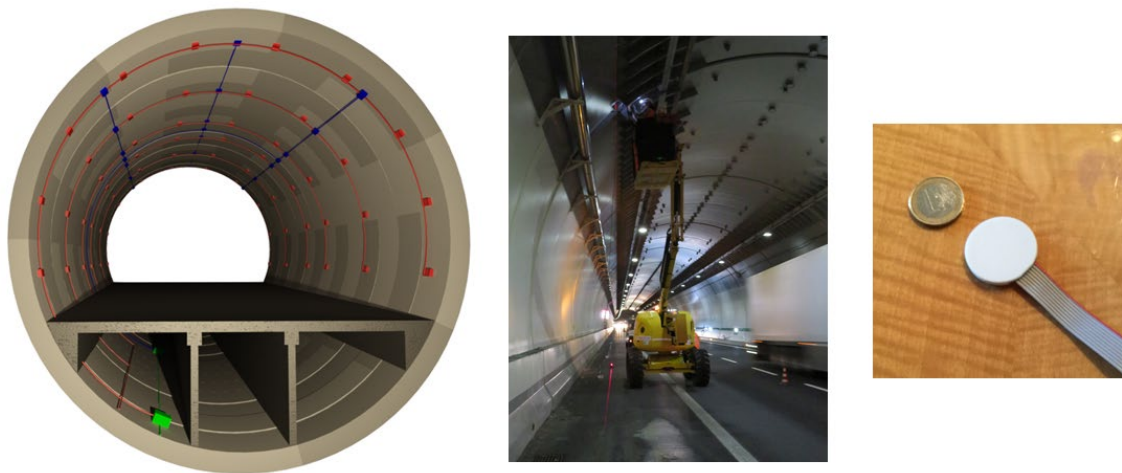


**Figure 1.** Monitoring system layout, installation, pressure sensor

In the present work we suppose to have installed 12 measuring points along each transverse section, which means one measuring point every  $30^\circ$ . Each measuring point will provide a value of rotation  $\phi$  (obtained from the clinometer) and value of axial force,  $N$ , and bending moment,  $M$ , obtained by integration of the pressures measured by the pressure sensors.

The real installation on the field is based on having one monitored section every 25m of distance along the longitudinal axis of the tunnel for a total number of measuring points equal to 480 per km. Each measuring point counts one clinometer and two pressure sensors for a total of 1440 measures per

km. The frequency of acquisition can be chosen by the user with a default value of one reading every 15 minutes.

The aim of the algorithm is to calculate a set of radial and tangential pressures that applied to the lining from the ground, will reproduce the same rotations, and internal actions measured by the sensors.

This set of pressures is then used to calculate internal actions along the lining cross section providing the best interpolation between the values measured by the sensors (in the 12 measuring points).

Internal actions inside a generic structure are in equilibrium with external loads and represent a minimum internal elastic energy condition for the structure. It is therefore better calculate internal actions starting from external loads than using interpolation techniques between measured points, as these techniques may find solutions that are not associated to minimum energy and are therefore more demanding and stressing for the structure than the real condition.

#### **4. Model description and calibration gold standards**

This work is the first step in the evolution of the complete system, therefore the calibration of the procedure has been done on theoretical pressures that can be applied by the ground to the lining derived from bibliography considerations and not on real monitoring data as this work has been done before the installation of the monitoring system.

A circular cross section tunnel has been chosen with 6m radius and thickness of the lining equal to 0.7m. No joints between segments have been modelled to keep the model as simple as possible, therefore cast in situ hypothesis is followed even if the circular cross section is typical of segmental construction.

A very simple 2D finite element model of a ring section of the lining has been realised using 72 linear frame elements (one every 5°). The boundary conditions are created by a set of fictitious radial and tangential springs with a stiffness of 1000 kN/m. This set of springs has been chosen with very low stiffness as it does not influence the solution, being the external loads applied to the system self-equilibrated. The springs are placed only to avoid lability of the model. This model can be realised using whatever structural finite element software in commerce as it does not need any terrain modelling.

The simple 2D finite element model of the ring has been loaded with the self-equilibrated actions coming from a complete geotechnical analysis done with a software like FLAC or RS2 [13], [14]. Internal actions  $M$ ,  $N$  and rotation  $\phi$  of the lining have been calculated in the 72 frame elements. The values of  $M_s$ ,  $N_s$ ,  $\phi_s$  in the 12 measuring points have been taken from this solution. This step is used only to create a target to which the genetic algorithm should converge. This solution represent a possible set of readings that the sensors may acquire on the field. When the system is fully operative there will be no need to run a geotechnical analysis. Two different set have been used to test the algorithm against different conditions: the first shows a vertical ovalization of the lining due to high horizontal trust, whereas the second shows ovalization on rotation of the lining. This solutions represent our gold standards (GS1 and GS2) and are shown in figure 2.



**Figure 2.** Target deformed shapes of GS1 and GS2 used in calibration procedure

### 5. Genetic algorithm description

The genetic algorithm (GA) used in this paper is based on the former works of one of the authors [17], [18], [19]. The population of the algorithm is represented by the radial and tangential actions that the terrain exchanges with the lining. This set of load is divided into a hydrostatic part, which is the mean radial pressure associated to the depth of the centre of the lining from the surface, and a deviatoric part.

The deviatoric part, which is responsible of rotation and ovalization, is made of a set of three distributed loads applied to the complete perimeter of the lining and described by simple harmonic shape functions, plus two uniformly distributed radial loads and two uniformly distributed tangential loads applied only to small segments of the lining. This loads are presented in table 1. Figure 3 represents the basic harmonic loads in non-dimensional space for a phase equal to zero.

**Table 1.** Harmonic shape functions for deviatoric load applied to lining.

Radial load	Tangential load
Harmonic loads	
$Nr_a(\varphi) = Ar_a(1 + \cos(\theta_{ra} + \varphi))$	$Nt_a(\varphi) = At_a \cdot \cos(0.5(\theta_{ta} + \varphi))$
$Nr_b(\varphi) = Ar_b(1 - \cos(2\theta_{rb} + 2\varphi))$	$Nt_b(\varphi) = At_b \cdot \sin(\theta_{tb} + \varphi)$
$Nr_c(\varphi) = Ar_c(1 + \cos(\theta_{rc} + \varphi))$	$Nt_c(\varphi) = At_c \cdot \sin(2\theta_{tc} + 2\varphi)$
Uniformly distributed loads	
$Nr_d(\varphi) = Ar_d \quad \text{if } \theta_{rd} - 15^\circ < \varphi < \theta_{rd} + 15^\circ$	$Nt_d(\varphi) = At_d \quad \text{if } \theta_{td} - 15^\circ < \varphi < \theta_{td} + 15^\circ$
$Nr_e(\varphi) = Ar_e \quad \text{if } \theta_{re} - 15^\circ < \varphi < \theta_{re} + 15^\circ$	$Nt_e(\varphi) = At_e \quad \text{if } \theta_{te} - 15^\circ < \varphi < \theta_{te} + 15^\circ$

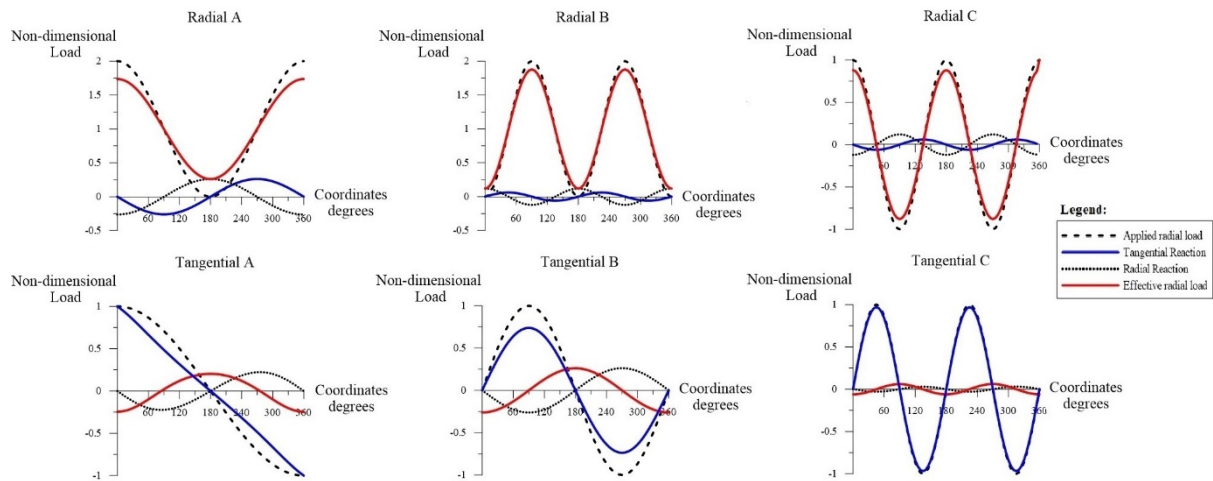


**Figure 3.** Harmonic loads and virtual spring reactions

The radial coordinate that identifies one point on the lining is called  $\varphi$  ( $0 < \varphi < 360^\circ$ ) and the meaning of the other symbols presented in table 1 is explained in table 2. The twenty values listed in table 2 are also the genes that constitute a generic individual of the population.

**Table 2.** Meaning of symbols.

Symbol	Meaning
$Ar_a, Ar_b, Ar_c$	Maximum magnitude of harmonic radial loads
$At_a, At_b, At_c$	Maximum magnitude of harmonic tangential loads
$\theta_{ra}, \theta_{rb}, \theta_{rc}$	Phases of harmonic radial loads
$\theta_{ta}, \theta_{tb}, \theta_{tc}$	Phases of harmonic tangential loads
$Ar_d, Ar_e$	Magnitude of uniform radial loads
$At_d, At_e$	Magnitude of uniform tangential loads
$\theta_{rd}, \theta_{re}$	Phases of uniform radial loads
$\theta_{td}, \theta_{te}$	Phases of uniform tangential loads

Different choices of the parameters listed in table 2 can yield to strongly different internal actions and rotations  $M_s, N_s, \theta_s$  in the 12 measuring points on the lining. The goal of the GA is to choose the configuration that minimizes the difference from the measured quantities and the numerical ones. Since the GA is a heuristic technique, the solution found can be a local minimum and not necessarily the global one, and anyway it is not able to prove the optimality of the solution.

As other population based methods, genetic algorithms are iterative solution techniques that handle a population of individuals and make them evolving according to some rules that have to be clearly specified. At each iteration, periods of self-adaptation alternate with periods of co-operation. Self-adaptation means that the individuals evolve independently while cooperation implies an exchange of information among the individuals.

The choice of a proper initial population plays a crucial role in the performance of a GA. In fact, if individuals belonging to the initial population are too much similar among each others, also the new generations would continue to be too much homogeneous, yielding to an exploration of only a small part of the solution space, with a great probability of remaining trapped in a local minimum. On the other hand, starting with individuals very different among each others but with a poor quality of the related solution could imply a very slow convergence of the algorithm to good quality solutions.

At each iteration, new individuals are created and it has to be decided which ones will enter the population itself. Moreover, individuals must be thrown out of the population in order to avoid a continuous expansion of it.

The choice of individuals which may reproduce themselves is taken according to a probability distribution related to a fitness function, which is based on the quality of the solution related to the individual, such that individuals corresponding to more promising solutions (let say “better individuals”) have a larger probability of reproduction as in the rules followed by the species evolution in nature and sciences. The fitness function used in this application is described by equations (1) to (4):

$$\text{Local error on measured quantity } X: \quad e_{M,i} = \left| \frac{X_{s,i} - X_{g,i}}{\bar{X}} \right| \quad (1)$$

$$\text{where:} \quad \bar{X} = \frac{\sum_{i=1}^n |X_{s,i}|}{n} \quad (2)$$

$$\text{Total error related to quantity } X: \quad e_X = \sum_{i=1}^n e_{X,i} \quad (3)$$

$$\text{Score related to quantity } X: \quad S_X = \frac{1}{e_X} \quad (4)$$

Where the quantity  $X$  can be  $N$ ,  $M$  or  $\phi$ . Each measuring station is identified by the subscript  $i$  ( $i = 1$  to  $n$  and  $n = 12$  in this case). The measured quantity by the sensor in each station is  $X_{s,i}$  and the corresponding value obtained in the station on the f.e.m model loaded with the individual  $j$  is  $X_{g,i}$ .

The total score of each individual  $j$  is given by equation (5)

$$S_j = \frac{1}{e_M + e_N + e_\phi} \quad (5)$$

When the fitness function is valued for all the  $N_{pop}$  individuals of the population, the selection of the individuals that will participate to the reproduction is done by the mechanism of the Russian Wheel.

The probability of being chosen for each individual is

$$p_j = \frac{S_j}{\sum_{j=1}^{N_{pop}} S_j} \quad (6)$$

Once two individuals  $j$  and  $k$  are chosen to be the parents of a new family, six new individuals are generated as follows:

1. same phases  $\theta$  of mother and mean of magnitudes  $A$  of mother and father;
2. same phases  $\theta$  of father and mean of magnitudes  $A$  of mother and father;
3. same magnitudes  $A$  of mother and mean of phases of mother and father;
4. same magnitudes  $A$  of father and mean of phases of mother and father;
5. mean of both magnitudes  $A$  and phases  $\theta$  of father and mother;
6. weighted mean of magnitudes  $A$  and phases  $\theta$  of father and mother as a function of the score of the parents (the parents with higher score gets higher weight).

Each family is therefore made of 8 individuals, two from the previous generation and six new. The individual with the highest score is chosen from each family. This reproduction procedure is repeated  $N_{pop}$  times in order to create a completely new generation.

## 6. Results and discussions

On both gold standard benchmarks GS1 and GS2 have been performed the tests described in the following paragraphs. Three values of the number of individuals in the population  $N_{pop}$  have been chosen: 24, 48 and 72 individuals. This choice has been done to analyse if the number of the individuals had a relevant role on the score obtained at the end of the process.

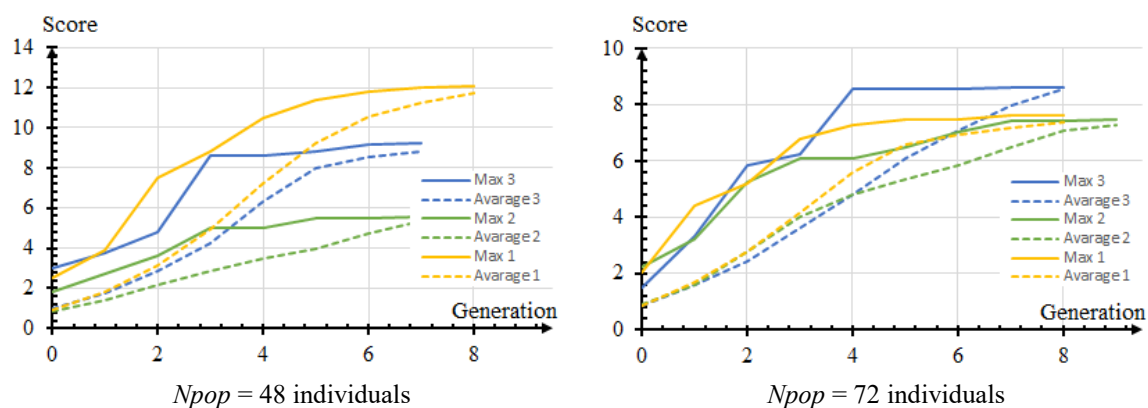
Two different batteries of three test each have been performed for each dimension of the starting population for each gold standard. The first battery starts always with the same starting population, whereas the second battery changes the initial population at of each test. This choice has been done to measure the amount of variability introduced by the reproduction technique on the same starting population.

Figure 4 shows the evolution of the score of the best individual of the population and the average score of the population through the generations for GS1, 48 and 72 individuals populations respectively, in the case in which the initial population is randomly changed at the beginning of each test.

It can be appreciated that the average starting score is in all 6 cases around 1, whereas the end score is always above 5 with a maximum of 12. At the end of the iterations the average score of the population is close to the maximum one as the procedure is not able to increase any more the value of the result having converged to an almost homogeneous population. The mean value of the maximum score is 8.96 for 48 individuals and 7.90 for 72 individuals. No much difference in average result can be appreciated between the two initial population's dimensions, whereas the population of 72 individuals shows less scattering, therefore better accuracy of each single test.

Table 3 shows the best individual results at the end of the process for all the test. It can be seen that GS2 suffered from poorer accuracy of the algorithm than GS1, being a more complex situation than GS1. It can also be seen that high variability in the final result is related to the starting populations; a guided choice of the individuals that constitute the initial population (instead of a full random one) is therefore needed to achieve best results.

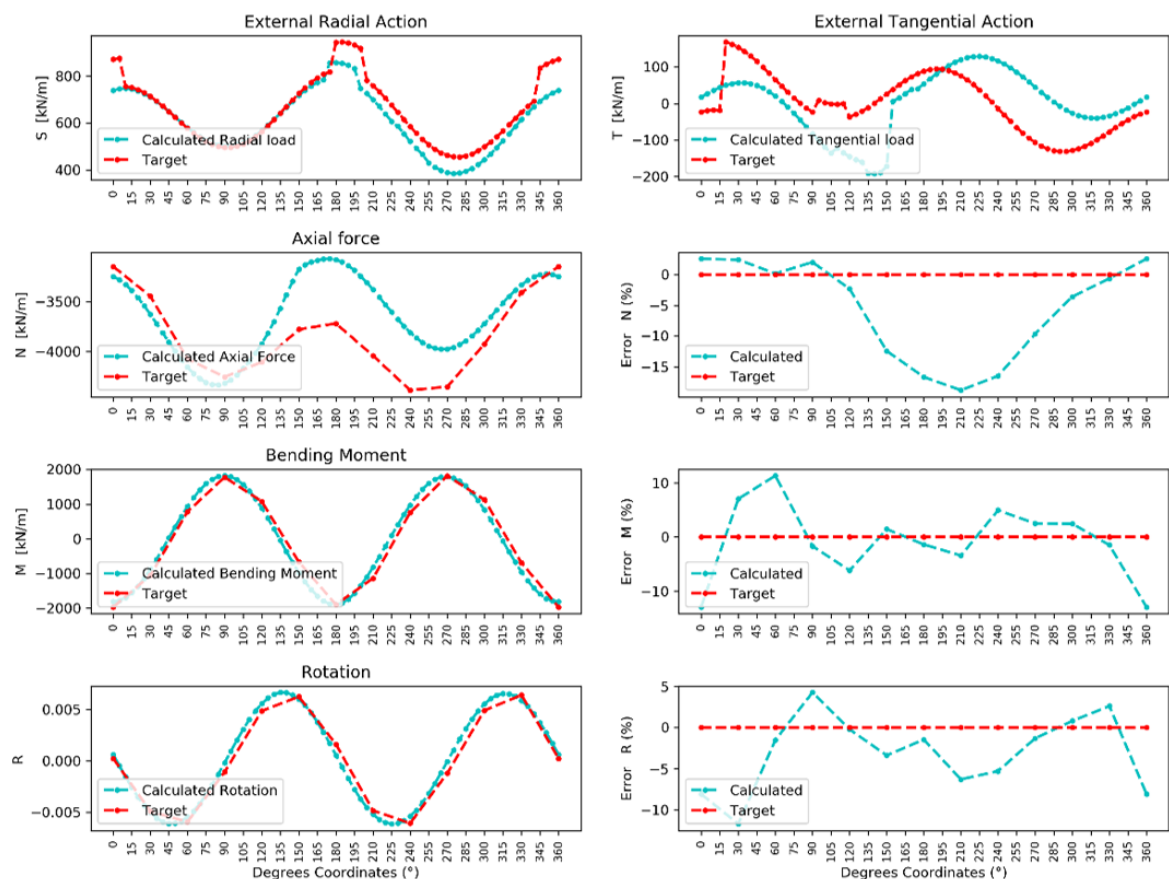
Figure 5 shows the comparison between the best result obtained for GS1 and the gold standard. Very good accuracy in the prediction of banding moment and rotation is appreciated (errors within  $\pm 10\%$ ), whereas lower accuracy is obtained on axial force and tangential stresses.



**Figure 4.** Evolution of mean and max score for GS1, new population for each test.

**Table 3.** Best individuals results at end of process

$N_{pop}$	Test number	GS1 Score		GS2 Score	
		Same starting population	New starting population	Same starting population	New starting population
24	1	9.29	3.36	3.94	1.49
	2	11.5	4.73	1.84	1.79
	3	5.56	7.08	1.35	3.32
	<b>Average</b>	<b>8.77</b>	<b>5.06</b>	<b>2.38</b>	<b>2.20</b>
48	1	10.7	12.1	4.01	6.54
	2	7.55	5.57	5.79	4.69
	3	9.39	9.20	4.24	4.39
	<b>Average</b>	<b>9.19</b>	<b>8.96</b>	<b>4.68</b>	<b>5.20</b>
72	1	10.0	8.60	7.96	3.43
	2	9.69	7.46	7.82	6.22
	3	11.0	7.64	7.71	4.92
	<b>Average</b>	<b>10.2</b>	<b>7.90</b>	<b>7.83</b>	<b>4.86</b>

**Figure 5.** Best score result for GS1

## 7. Conclusions

An application of genetic algorithms to tunnel monitoring is presented in this paper. Good accuracy and results are achieved, but the need of a guidance in the choice of the initial population is clearly emerged. Further development of the present work will be the refinement of the shape functions of the external load calibrating them on geotechnical simulations and the use of proper guidance in the choice of the initial population to feed the GA.

## References

- [1] G.N. Pande, G. Beer and J.R. Williams, "Numerical Methods in Rock Mechanics", John Wiley and Sons, Ltd, 1990.
- [2] J.M. Duncan and C.Y. Chang, "Nonlinear analysis of stress and strain in soils", *J. of Soil Mech. and Foundation Division*, ASCE, vol. 96, No SM 5, pp: 1629-1653, 1970.
- [3] N. Do and D. Dias, "Tunnel lining design in multi-layered grounds", *Tunnelling and Underground Space Technology*, vol. 81, pp: 103-111, 2018.
- [4] P. Castaldo and M. De Iuliis, "Effects of deep excavation on seismic vulnerability of existing reinforced concrete framed structures", *Soil Dynamics and Earthquake Engineering*, vol. 64, pp: 102-112, 2014.
- [5] P. Castaldo, F. Jalayer and B. Palazzo, "Probabilistic assessment of groundwater leakage in diaphragm wall joints for deep excavations", *Tunnelling and Underground Space Technology* vol. 71, pp: 531-543, 2018.
- [6] P. Castaldo, M. Calvello and B. Palazzo, "Probabilistic analysis of excavation-induced damages to existing structures", *Computers and Geotechnics*, vol. 53, pp: 17-30, 2013.
- [7] C. R. Farrar and K. Worden, "Structural Health Monitoring, a Machine Learning Perspective", John Wiley & Sons, 2013, ISBN: 978-1-119-99433-6.
- [8] D. Balageas, C.-P. Fritzen and A. Güemes: "Structural Health Monitoring" Wiley, 2006, ISBN: 9781905209019.
- [9] C. Boller, F.-K. Chang, Y. Fujino, "Encyclopedia of Structural Health Monitoring", Wiley, 2009, ISBN: 978-0-470-05822-0.
- [10] N. Do, D. Dias, P. Oreste and I. D. Maigre, "2D numerical investigation of segmental tunnel lining behaviour", *Tunnelling and Underground Space Technology*, vol 37, August 2013, pp: 115-127, 2013.
- [11] N. Vlachopoulos and M. S. Diederichs, "Improved Longitudinal Displacement Profiles for Convergence Confinement Analysis of Deep Tunnels", *Rock Mech Rock Engng*, vol. 42, pp: 131-146, 2009.
- [12] FLAC Version 8.0 User's Guide, Itasca Consulting Group, Inc. Minneapolis, USA, 2019.
- [13] RS2 2019 User's Manual, Rocscience, Toronto, Canada, 2019.
- [14] K. FiferBizjak and B. Petkovšek, "Displacement analysis of tunnel support in soft rock around a shallow highway tunnel at Golovec", *Engineering Geology*, vol. 75, Issue 1, pp: 89-106, 2004.
- [15] Y. Zhang, J. Yang and F. Yang, "Field investigation and numerical analysis of landslide induced by tunnelling", *Engineering Failure Analysis*, vol. 47, Part A, pp: 25-33, 2015.
- [16] L. Noferinia, M. Pieraccini, D. Mecatti, G. Macaluso, C. Atzeni, M. Mantovani, G. Marcato, A. Pasuto, S. Silvano and F. Tagliavini, "Using GB-SAR technique to monitor slow moving landslide", *Engineering Geology*, vol. 95, Issues 3-4, pp: 88-98, 2007.
- [17] G. Bertagnoli, L. Giordano and S. Mancini, "Design and optimization of skew reinforcement in concrete shells", *Structural Concrete*, vol. 13 n. 4, pp: 248-258, 2012.
- [18] G. Bertagnoli, L. Giordano and S. Mancini, "Optimization of concrete shells using genetic algorithms", *ZAMM - Journal of Applied Mathematics and Mechanics / Zeitschrift für Angewandte Mathematik und Mechanik*, vol. 94 n. 1-2, pp: 43-54, 2014.
- [19] G. Bertagnoli, L. Giordano, and S. Mancini, "A Metaheuristic Approach to Skew Reinforcement Optimization in Concrete Shells Under Multiple Loading Conditions", *Structural Engineering International*, vol. 24 n. 2, pp: 201-210, 2014.